This is the accepted manuscript made available via CHORUS. The article has been published as:

Examining the role of transfer coupling in sub-barrier fusion of ^{46,50}Ti+^{124}Sn

J. F. Liang (□□□), J. M. Allmond, C. J. Gross, P. E. Mueller, D. Shapira, R. L. Varner, M. Dasgupta, D. J. Hinde, C. Simenel, E. Williams, K. Vo-Phuoc, M. L. Brown, I. P. Carter, M. Evers, D. H. Luong, T. Ebadi, and A. Wakhle

Phys. Rev. C **94**, 024616 — Published 24 August 2016

DOI: 10.1103/PhysRevC.94.024616

Examining the role of transfer coupling in sub-barrier fusion of ^{46,50}Ti+^{124}Sn*

J.F. Liang (梁君健)†, J.M. Allmond, C.J. Gross, P.E. Mueller, D. Shapira, R.L. Varner

Physics Division, Oak Ridge National Laboratory, Oak Ridge, Tennessee 37831, USA

M. Dasgupta, D.J. Hinde, C. Simenel, E. Williams, K. Vo-Phuoc, M.L. Brown, I.P. Carter, M. Evers‡, D.H. Luong, T. Ebadi§, A. Wakhle¶

Department of Nuclear Physics, Research School of Physical Sciences and Engineering, The Australian National University, Canberra, ACT 2601, Australia

Abstract

Background The presence of neutron transfer channels with positive Q-values can enhance sub-barrier fusion cross sections. Recent measurements of the fusion excitation functions for ^{58}Ni+^{132,124}Sn found that the fusion enhancement due to the influence of neutron transfer is smaller than that in ^{40}Ca+^{132,124}Sn although the Q-values for multineutron transfer are comparable. **Purpose** To investigate the differences observed between the fusion of Sn+Ni and Sn+Ca. **Methods** Fusion excitation functions for ^{46,50}Ti+^{124}Sn have been measured at energies near the Coulomb barrier. **Results** A comparison of the barrier distributions for ^{46}Ti+^{124}Sn and ^{40}Ca+^{124}Sn shows that the ^{40}Ca+^{124}Sn system has a barrier strength resulting from the coupling to the very collective octupole state in ^{40}Ca at an energy significantly lower than the uncoupled barrier. **Conclusions** The large sub-barrier fusion enhancement in ^{40}Ca induced reactions is attributed to both couplings to neutron transfer and inelastic excitation, with the octupole vibration of ^{40}Ca playing a major role.

PACS numbers: 25.70Gh,25.70Jj,24.10Eq

* This manuscript has been authored by UT-Battelle, LLC, under Contract No. DE-AC05-00OR22725 with the U.S. Department of Energy. The United States Government retains and the publisher, by accepting the article for publication, acknowledges that the United States Government retains a nonexclusive, paid-up irrevocable, worldwide license to publish or reproduce the published form of the manuscript, or allow others to do so, for United States Government purposes.

† Present address: FLIR Systems Inc., USA

‡ Present address: John Curtin School of Medical Research, ANU, Canberra, Australia

§ Present address: Seeing Machines, Canberra, Australia

¶ Present address: National Superconducting Cyclotron Laboratory, MSU, USA

I. INTRODUCTION

Heavy-ion fusion near the Coulomb barrier continues to attract experimental and theoretical interest [1]. The enhanced fusion cross sections at sub-barrier energies, with respect to a one-dimensional barrier penetration model, can be described by the coupling of the relative motion to the internal degrees of freedom of the participants. The coupling to neutron transfer may be important for reactions involving neutron-rich radioactive nuclei because for some projectile and target combinations there are a large number of positive Q-value transfer channels. This is particularly interesting for the synthesis of superheavy elements since neutron-rich radioactive beams may ultimately be used for such experiments [2]. Moreover, neutron transfer is predicted to enhance the fusion of neutron-rich nuclei occurring in the crust of accreting neutron stars [3]. These fusion reactions may affect the temperature profile and compositions of neutron stars [4]. Therefore, it is essential to understand the effect of transfer couplings on sub-barrier fusion.

The measurement of the fusion excitation function for ^{40}Ca+^{132}Sn found a very large sub-barrier fusion enhancement compared to the fusion of ^{48}Ca+^{132}Sn [5]. Coupled-channels calculations considering the inelastic excitations to the lowest 2^+ and 3^- states of the participating nuclei were able to reproduce the excitation function for ^{48}Ca+^{132}Sn but severely underpredicted the excitation function for ^{40}Ca+^{132}Sn. Because the Q-values for ground-state transfer of up to 14 neutrons from ^{132}Sn to ^{40}Ca are positive and all the ground state to ground-state transfer Q-values (Q_{gg}) for ^{48}Ca+^{132}Sn are negative, the large sub-barrier fusion enhancement in ^{40}Ca+^{132}Sn was attributed to the couplings to transfer [5]. Likewise, a large sub-barrier fusion enhancement observed in ^{40}Ca+^{134}Te was also attributed to the same mechanisms [6]. The interpretation of these measurements is supported by the stable beam experiment studying the fusion of ^{40}Ca and ^{124}Sn, which exhibits a very large sub-barrier fusion enhancement [7]. The presence of multineutron transfer with positive Q-values suggests that transfer plays a very important role. Furthermore, this observation is similar to the work which compared the fusion excitation functions for ^{40}Ca+^{90,94,96}Zr [9]. The fusion excitation function for ^{40}Ca+^{90}Zr was reproduced by coupled-channels calculations including the inelastic excitation of the projectile and target. However, similar calculations underpredicted the sub-barrier fusion cross sections for ^{40}Ca+^{94,96}Zr. The large sub-barrier fusion enhancement was attributed to the coupling to neutron transfer in ^{40}Ca+^{94,96}Zr because of the large positive Q-values [8, 9]. Nevertheless, the sub-barrier fusion enhancement for ^{40}Ca+^{132}Sn appears to be no larger than that for ^{40}Ca+^{124}Sn even though the Q-values for neutron transfer are larger for ^{40}Ca+^{132}Sn.

The fusion excitation function for ^{58}Ni+^{132}Sn [10] has been compared with ^{64}Ni+^{124,132}Sn [11], ^{58}Ni+^{124}Sn, and ^{64}Ni+^{118}Sn [12]. The number of neutron transfer channels with positive Q-values and the magnitude of the Q-values differ significantly among these systems, but there is no noticeable difference in sub-barrier fusion enhancement [10]. Moreover, when the differences in nuclear size and the barrier height are factored out, the fusion excitation functions for Sn+Ni overlap with that for ^{48}Ca+^{132}Sn which has no positive Q-values for transfer. The heavier systems ^{58,64}Ni+^{130}Te also exhibit similar behavior where the sub-barrier fusion enhancement shows no correlation with neutron transfer.

Recently, the measurement of the fusion cross sections for ^{58,64}Ni+^{124}Sn was extended to cross sections down to 1 μb [13]. A comparison of the two excitation functions shows that the sub-barrier fusion enhancement for ^{58}Ni induced fusion becomes larger than that for ^{64}Ni induced fusion at cross sections less than 1 mb. The fall-off of the excitation function

becomes less steep for ^{58}Ni+^{124}Sn also. The analysis of the neutron transfer Q-values and coupled-channels calculations show that the sub-barrier fusion enhancement in ^{58}Ni+^{124}Sn is influenced by neutron transfer.

However, for ^{40}Ca induced reactions, the influence of transfer on sub-barrier fusion is visible at cross sections of a few tens of millibarns when the excitation functions are compared with fusion induced by ^{48}Ca. For ^{58}Ni induced reactions, the influence of transfer on sub-barrier fusion is not visible until cross sections as small as 1 mb, even though the magnitude of Q-values for transfer are similar and the number of channels with positive transfer Q-value are comparable to ^{40}Ca induced fusion. Therefore, it is necessary to further investigate the influence of transfer on sub-barrier fusion, particularly, the different behaviors between ^{40}Ca and ^{58}Ni induced fusion.

There are a few differences between the two reaction sets, Sn+Ni and Sn+Ca. The product of the atomic number for the projectile and target, $Z_P Z_T$, is 1000 for Sn+Ca and 1400 for Sn+Ni. Because of the larger $Z_P Z_T$ for Sn+Ni, deep inelastic collisions may influence the sub-barrier fusion process [14]. In addition, the open orbitals for neutrons transferring from Sn to Ca are $f_{7/2}$ and above, whereas the open orbitals for neutrons transferring from Sn to Ni are $p_{3/2}$ and above. The form factor for neutron transfer depends on the angular momentum of the initial and final states. This may result in different coupling strengths, therefore, leading to the differences in sub-barrier fusion enhancement observed between the two systems. Furthermore, the ^{40}Ca nucleus has a very collective octupole state at 3.74 MeV. The coupling of the excitation to this state has been shown to have a considerable influence on sub-barrier fusion [15].

In order to further explore the transfer couplings and try to resolve the differences observed in the sub-barrier fusion enhancement in Ca+Sn and Ni+Sn, the fusion cross sections for ^{46,50}Ti+^{124}Sn have been measured. The $Z_P Z_T$ for Sn+Ti is 1100, for which the deep inelastic scattering cross section is expected to be small and comparable to that for ^{40}Ca+^{124}Sn. The Q-values for transferring two to five neutrons in ^{46}Ti+^{124}Sn are similar to those in ^{40}Ca+^{124}Sn, as shown in Fig. 1. The $f_{7/2}$ orbital in ^{46}Ti is half filled. The remaining $f_{7/2}$ orbital would accommodate some of the neutrons transferring from Sn to ^{46}Ti. These aspects of the reaction are similar to ^{40}Ca+^{124}Sn. However, the excitation property for the lowest octupole state in ^{46}Ti is more similar to that in ^{58}Ni. As a reference, the ^{50}Ti+^{124}Sn reaction was measured because there is no positive Q-value for neutron transfer.

II. EXPERIMENT

The first experiment was performed at the Holifield Radioactive Ion Beam Facility (HRIBF) at Oak Ridge National Laboratory. The ^{124}Sn beams were accelerated by the 25 MV tandem electrostatic accelerator to energies near the Coulomb barrier. The targets were self-supporting metallic foils with thickness of 295 μg/cm^2 for ^{46}Ti and 270 μg/cm^2 for ^{50}Ti. The compound nucleus decayed predominantly by particle evaporation. Fission was estimated by the statistical model code EVAPOR [16] to be negligible until beam energies 10 % above the barrier, as shown by the dotted curves in Fig. 2. Because the comparison of the fusion excitation functions are important only for energies near and below the barrier, the fission expected at higher energies need not be considered. For this reason, the evaporation residue (ER) cross sections are taken as the fusion cross sections at energies near and below the barrier. The ERs were identified by time-of-flight using microchannel-plate timing detectors and energy loss using a multi-anode ionization chamber. A detailed description of

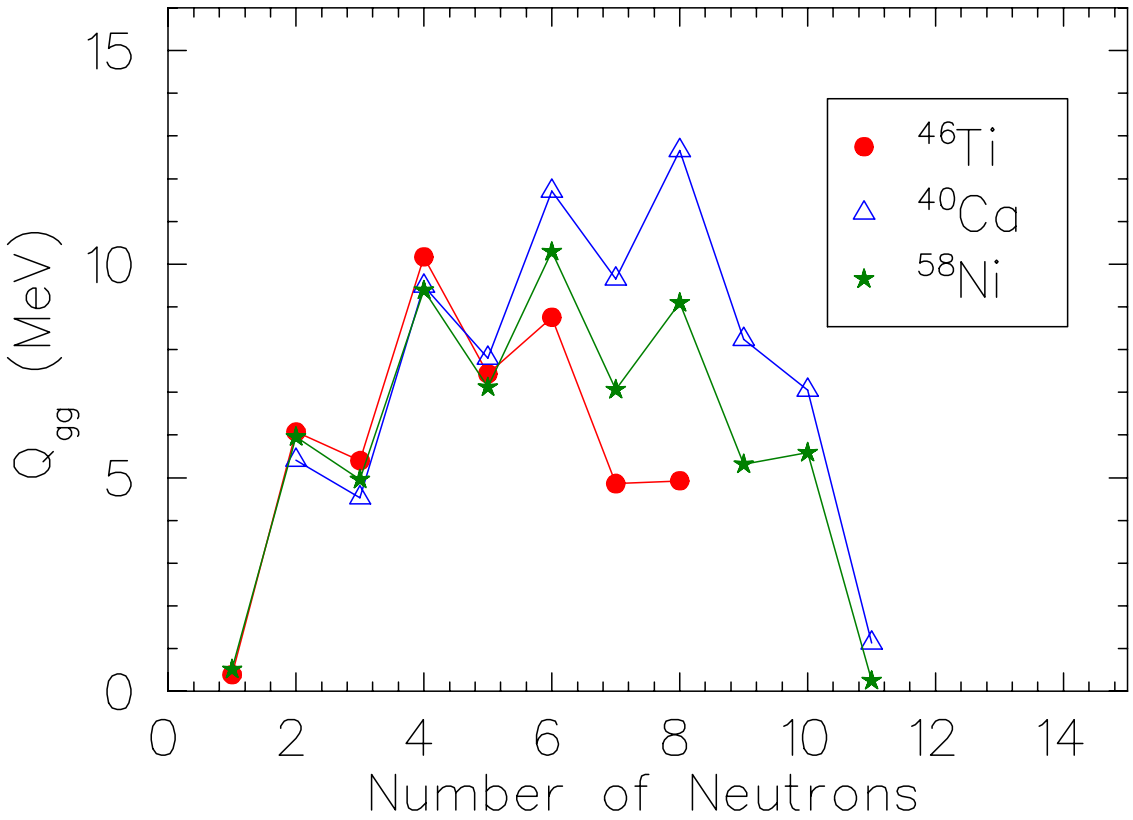

FIG. 1: (Color online) Ground-state Q-values as a function of the number of neutrons picked up by ^{46}Ti and ^{40}Ca from ^{124}Sn. Only the channels with positive Q-values are shown. The filled circles are for ^{46}Ti+^{124}Sn, the open triangles are for ^{40}Ca+^{124}Sn, and the solid stars are for ^{58}Ni+^{124}Sn.

the apparatus can be found in Ref. [17].

A follow-up measurement was carried out at the Australian National University (ANU). The objective was to measure fusion cross sections to high precision with an energy step of 1.4 MeV to allow determination of the experimental barrier distribution. The ^{46,50}Ti beams were accelerated by the 14UD tandem electrostatic accelerator. Two sandwiched targets of 17 μg/cm^2 ^{124}Sn evaporated onto 20μg/cm^2 carbon backings were used. The ERs were transported in the superconducting solenoid, SOLITAIRE, and detected by two multiwire proportional counters at and behind the focus [18]. In order to maintain the ER transmission and beam particle rejection SOLITAIRE was filled with 1 Torr of helium gas. The magnetic field was set at 5.5 Tesla throughout the measurements. The efficiency of the device was simulated by a Monte Carlo program developed at ANU [19]. To calibrate the simulation, the ^{34}S+^{89}Y reaction was used since the angular distributions of the ERs and the fusion cross sections were measured and published [20]. The calculated efficiency for transmission and detection of all the ERs varied from 58% at the lowest energy to 73% at the highest energy. Four silicon detectors located at 18° surrounding the beam axis were used to detect the elastically scattered beam particles for cross section normalization.

III. RESULTS

Fig. 2 presents the ER cross sections as a function of the center-of-mass energy for ^{46,50}Ti+^{124}Sn. The HRIBF data are shown by the solid circles and the ANU measurements are shown by the crosses. The two measurements for ^{46}Ti+^{124}Sn are in good agreement.

Next, theoretical predictions are compared with the data. One of the most important inputs to both no-coupling and coupled-channels calculations is the nuclear potential. Commonly used phenomenological potentials, obtained from fits to experimental data, implicitly include the effects of couplings to states at high excitation energies which could lead to a potential shift. Given that this work is aimed at investigating the interplay of couplings to transfer and inelastic channels, the nuclear potential should be free of coupling effects, *i.e.*, the "bare" nuclear potential should be chosen. Therefore, the frozen Hartree-Fock (HF) technique was used to obtain the nuclear potential [30]. The frozen HF potential has no free parameters that change from system to system, is self consistent, and gives the "bare" nuclear potential. The choice of frozen HF potential is discussed further in the next section.

The predictions of the one-dimensional barrier penetration model (uncoupled) using the frozen HF nuclear potential are shown by the dashed curves. At high energies, the measured ER cross sections are smaller than the prediction of the uncoupled calculation. This is due to the fact that the fission decay of the compound nucleus was not measured. Statistical model calculation using the code EVAPOR is able to reproduce the measured ER cross sections. Furthermore, the calculation shows that the fission contribution to the fusion cross section gets smaller as the reaction energy decreases. It becomes negligible at energies near and below the barrier which is the focus of this work. It can be seen that there is a large sub-barrier fusion enhancement for both reaction systems compared with the no-coupling calculations. The enhancement for ^{46}Ti+^{124}Sn is larger than that for ^{50}Ti+^{124}Sn.

The results of coupled-channels calculations, using the code CCFULL [21], including excitation of the projectile and target to the lowest 2^+ and 3^- states are shown by the solid curves in Fig. 2. For these calculations, the excitation energies and deformation parameters were obtained from the literature [27, 28] and given in Table I whereas the nuclear potentials deduced from the frozen HF technique are shown in Table II. In addition, two-phonon excitations including the mutual excitation of the projectile and target are considered. For the ^{50}Ti+^{124}Sn reaction, the lowest 4^+ state with an excitation of 2.68 MeV is assumed to be the double-phonon state in the calculation. Because the transition strength from the ground state has been measured, the direct transition to this state is included in the coupled-channels calculation. The calculation underpredicts the sub-barrier cross sections for ^{50}Ti+^{124}Sn. This underprediction may be the result of a positive Q-value for two-proton transfer. In contrast, there is a much larger discrepancy between the calculation and measurement for ^{46}Ti+^{124}Sn, particularly at cross sections less than 1 mb. The measured sub-barrier cross sections are much larger than the calculation, as seen by the increasing deviation from the solid curve in Fig. 2(a). In order to compare the underprediction by the coupled-channels calculations for these two reactions, the calculated cross sections subtracted from the measured cross sections at energies below the barrier are shown in Fig. 3. As can be seen, the discrepancy between measurement and calculation is small for ^{50}Ti+^{124}Sn. Conversely, the discrepancy between experimental data and the calculation is quite large for ^{46}Ti+^{124}Sn. The presence of positive Q-value transfer channels in ^{46}Ti+^{124}Sn suggests that coupling to these channels may be important, similar to the fusion of ^{40}Ca with ^{124}Sn [7].

nucleus	E (MeV)	λ^π	β_λ
^{46}Ti	0.89	2^+	0.317
	3.06	3^-	0.142
^{50}Ti	1.55	2^+	0.166
	4.41	3^-	0.138
	2.68	4^+	0.050
^{124}Sn	1.13	2^+	0.095
	2.60	3^-	0.106

TABLE I: Nuclear structure parameters for CCFULL calculations. The β_λ is the deformation parameter for inelastic excitation couplings.

reaction	V (MeV)	$r_\circ$ (fm)	a (fm)
^{46}Ti+^{124}Sn	125	1.1487	0.6454
^{50}Ti+^{124}Sn	116	1.1534	0.6322

TABLE II: Bare nuclear potential for interaction between ^{46,50}Ti and ^{124}Sn. The frozen Hartree-Fock technique is used to generate the potential. Subsequently, the potential is fitted to the Woods-Saxon shape to deduce the potential depth V, the radius parameter $r_\circ$, and the diffuseness a.

IV. DISCUSSIONS

The magnitude of sub-barrier fusion enhancement among different reaction systems is customarily compared by plotting the fusion excitation functions in the same graph. For reactions with projectile and target of fixed atomic numbers but different isotopes, the differences in nuclear size and barrier height are little and a fair comparison is possible. However, when the comparison is made among reaction systems with projectile and target having different atomic numbers, it is necessary to account for the differences in nuclear size and barrier height. One of the usual ways to achieve that is through the use of reduced scales where the reaction energy is divided by the barrier height and the cross section is divided by the nuclear radius. There are several models that are developed to describe the nuclear potential between two nuclei. The barrier heights for ^{40,48}Ca+^{124}Sn, ^{46,50}Ti+^{124}Sn, and ^{58,64}Ni+^{124}Sn predicted by Broglia-Winther [22], Bass [23], and Sao Paulo [24] models are shown in Fig. 4. The comparison is made by scaling to the Coulomb energy $Z_P Z_T e^2/R$, where Z is the atomic number, e is the electric charge, and $R = 1.2(A_P^{1/3} + A_T^{1/3})$ is the radius with A being the nuclear mass. It can be seen that the predicted barrier heights agree for some reactions but differ for others. Additionally, there seems to be different correlations between the predicted barrier height and the Coulomb energy.

Since many of the models presented in Fig. 4 use parameters deduced from systematics, the difference in predictions may be, in part, due to the different reaction systems included in compiling the systematics. Thus, it is important to choose a model as a reference for comparison carefully. Moreover, as more experiments are performed with radioactive beams and reactions involving these nuclei are not included in obtaining the systematics, the uncertainty in the models could become large, particularly for nuclei very far from stability.

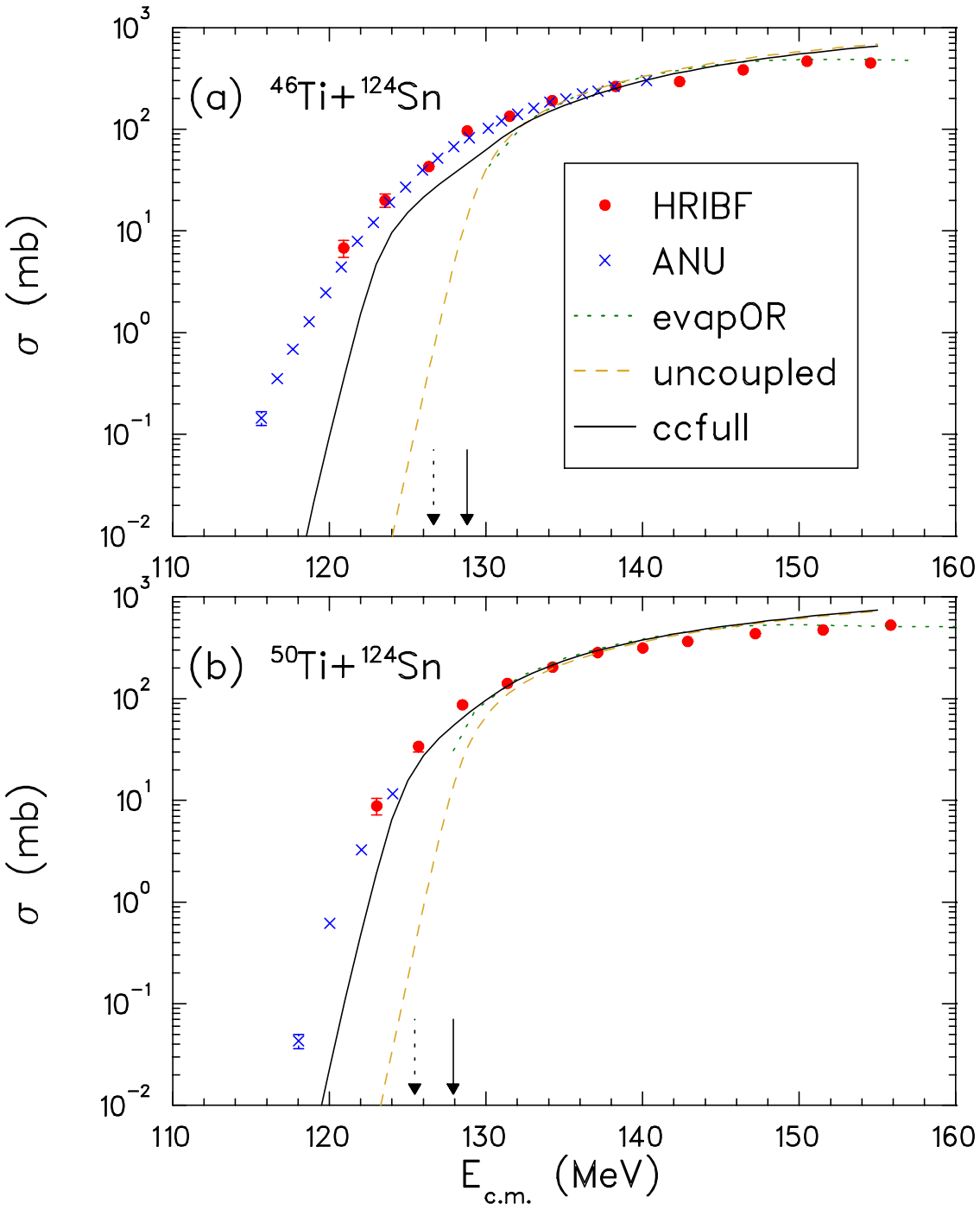

FIG. 2: (Color online) (a) Fusion excitation function for ^{46}Ti+^{124}Sn. The circles are for measurements performed in inverse kinematics at HRIBF and the crosses are for measurements carried out in normal kinematics at ANU. The dotted curve is for the ER cross sections predicted by the statistical model code EVAPOR. The result of a one-dimensional barrier penetration model calculation is shown by the dashed curve. The coupled-channels calculation including up to two-phonon excitations of the projectile and target are shown by the solid curve. The barrier height predicted by the frozen Hartree-Fock (HF) method is shown by the solid arrow whereas the barrier height predicted by the time-dependent Hartree-Fock method (TDHF) is shown by the dotted arrow. (b) Fusion excitation function for ^{50}Ti+^{124}Sn.

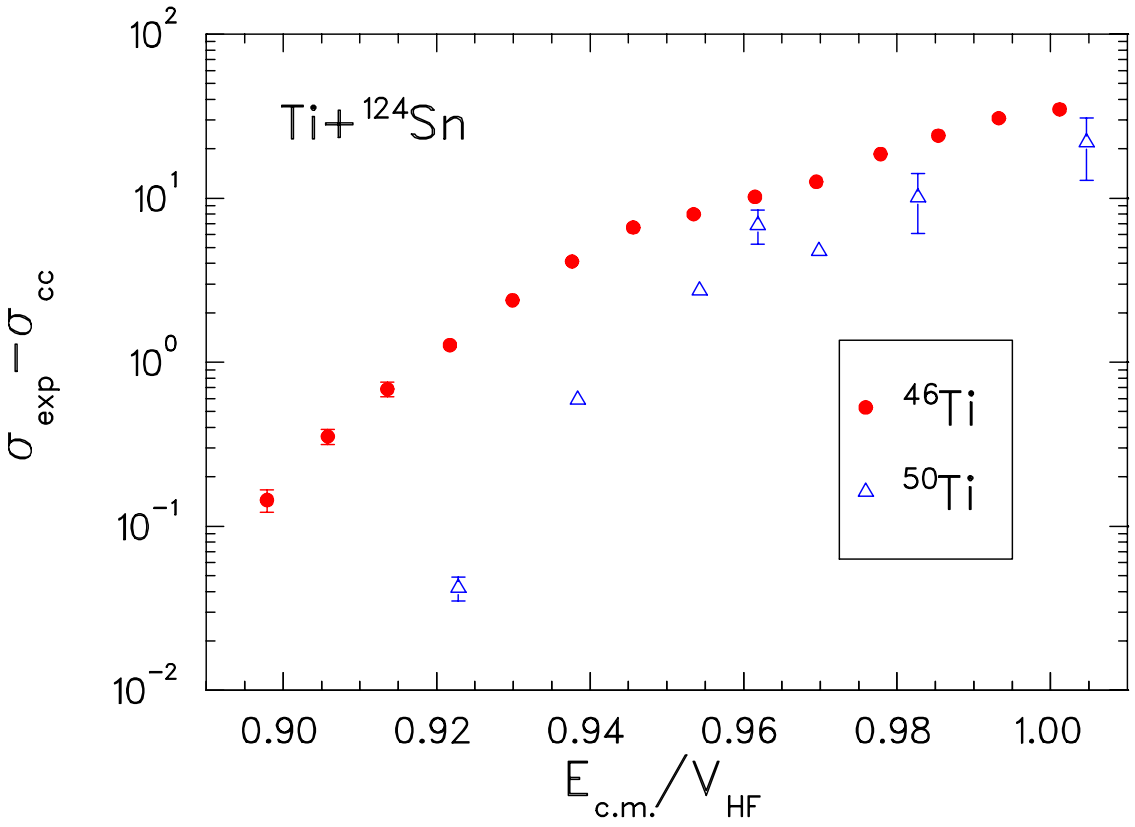

FIG. 3: (Color online) Fusion excitation functions calculated by CCFULL subtracted from those measured for $+^{46}$Ti+^{124}Sn (filled circles) and ^{50}Ti+^{124}Sn (open triangles).

In order to avoid making comparisons that depend on the variation in models, it would be advantageous to use a model that carries nuclear structure information. One such model is based on an energy density functional [25] which is consistent in describing nuclear structure and nuclear interaction under the assumption that the ground state densities are frozen. The latter are determined within the HF microscopic mean field approach. The HF method for modeling many-body systems has been successful for predicting nuclear structure properties. In this work, the frozen HF model is adopted for estimating the barrier height. The only input to the frozen HF is the energy density functional which is deduced from effective Skyrme nucleon-nucleon interaction. Because the HF technique properly accounts for the nuclear structure effects, the barrier height predicted is fairly different from the other three models which mostly rely on fitting heavy-ion reaction data from stable beam experiments. Moreover, the frozen HF method gives the "bare" barrier which is not influenced by potential shifts due to couplings to high lying collective states or a multitude of weak couplings.

In Fig. 5, the fusion excitation functions for (a) ^{40,48}Ca+^{96}Zr [8, 26], (b) ^{40,48}Ca+^{124}Sn [5], (c)^{40,48}Ca+^{132}Sn [5], (d) ^{46,50}Ti+^{124}Sn, (e)^{58,64}Ni+^{124}Sn [12, 13], and (f) ^{58,64}Ni+^{132}Sn [10, 11] are compared where the reaction energy is shown on a reduced scale using the barrier height predicted by the frozen HF. For ^{40}Ca induced reactions, the sub-barrier fusion enhancement is larger than for ^{48}Ca induced reactions, as seen in panels (a), (b), and (c). The difference is clearly visible at cross sections of several tens of millibarns. Because the Q-values for transferring a multiple number of neutrons from ^{96}Zr and ^{124,132}Sn to ^{40}Ca are positive whereas the Q-values for neutron transfer are negative for reactions involving ^{48}Ca,

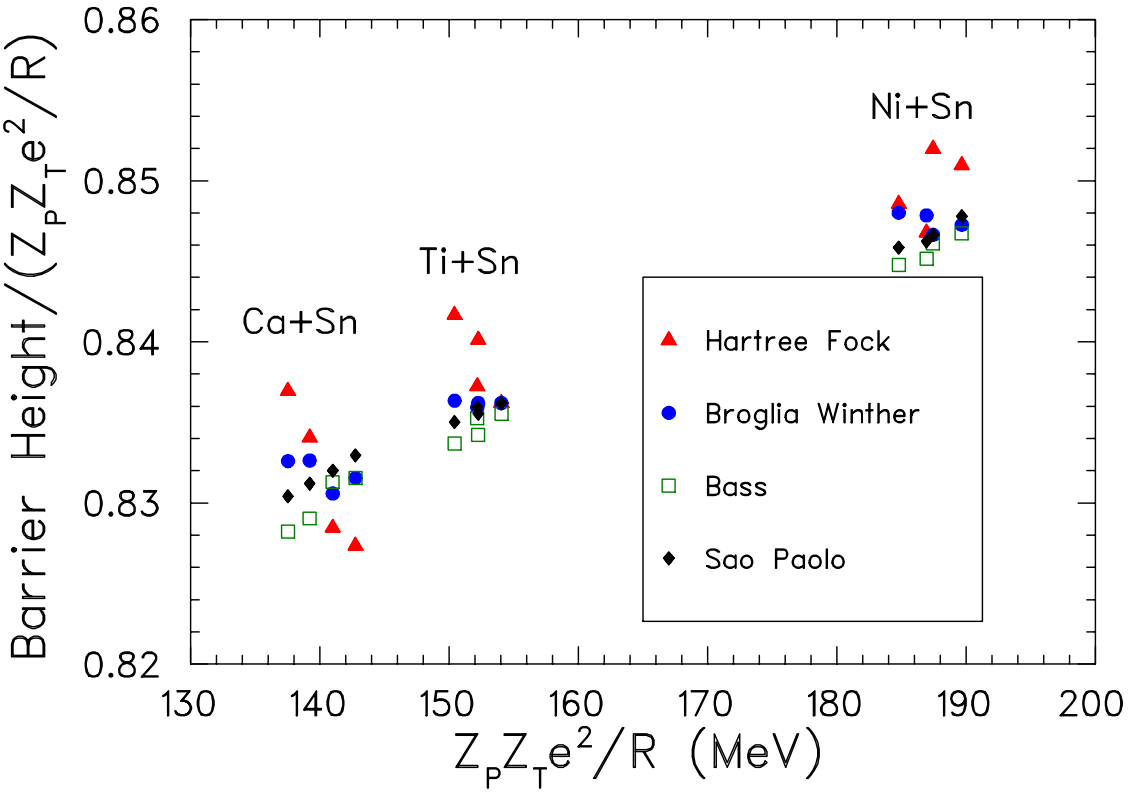

FIG. 4: (Color online) Reduced barrier height predicted by the frozen Hartree-Fock method (solid triangles), Broglia-Winther systematics (solid circles), Bass model (open squares), and Sao Paulo model (solid diamonds) as a function of $Z_P Z_T e^2/R$ for ^{40,48}Ca+^{124,132}Sn, ^{46,50}Ti+^{124,132}Sn, and ^{58,64}Ni+^{124,132}Sn.

the larger sub-barrier fusion enhancement has in the past been attributed to the coupling to neutron transfer [5, 7, 8, 26]. However, if the the same reasoning is applied to ^{58}Ni and ^{64}Ni induced fusion on ^{124}Sn and ^{132}Sn then the sub-barrier fusion enhancement is expected to be larger for ^{58}Ni induced reactions. As shown in Fig. 5(e), the sub-barrier fusion enhancement for ^{58}Ni+^{124}Sn is indeed larger than for ^{64}Ni+^{124}Sn, but the enhancement is smaller than for Ca and Ti induced reactions, and it is only clearly seen for cross sections less than 1 mb. Also shown in the figure is the fusion excitation function of ^{64}Ni+^{118}Sn (crosses) for which the Q-values for multineutron transfer are negative. At cross sections larger than 1 mb, these three excitation functions overlap with each other. Fig. 5(f) shows the measurements of ^{58,64}Ni+^{132}Sn. It was very difficult to measure cross sections below 1 mb at current radioactive beam facilities due to the low intensity. The reduced fusion excitation functions for ^{58}Ni+^{132}Sn and ^{64}Ni+^{132}Sn are similar and do not show the influence of multineutron transfer on sub-barrier fusion. Perhaps, at lower energies where the cross section is well below 1 mb the effects of multineutron transfer on sub-barrier fusion may appear.

The comparison of fusion excitation functions measured in this work, ^{46,50}Ti+^{124}Sn, is shown in Fig. 5(d). It can be seen that the sub-barrier fusion enhancement is larger for ^{46}Ti+^{124}Sn which has positive Q-values neutron transfer channels similar to ^{40}Ca+^{124}Sn. The difference becomes visible at cross sections greater than 10 mb, similar to ^{40}Ca induced fusion. To further examine whether there are differences between the fusion of Ca+Sn and Ti+Sn, the reduced excitation functions for the two systems are compared in Fig. 6.

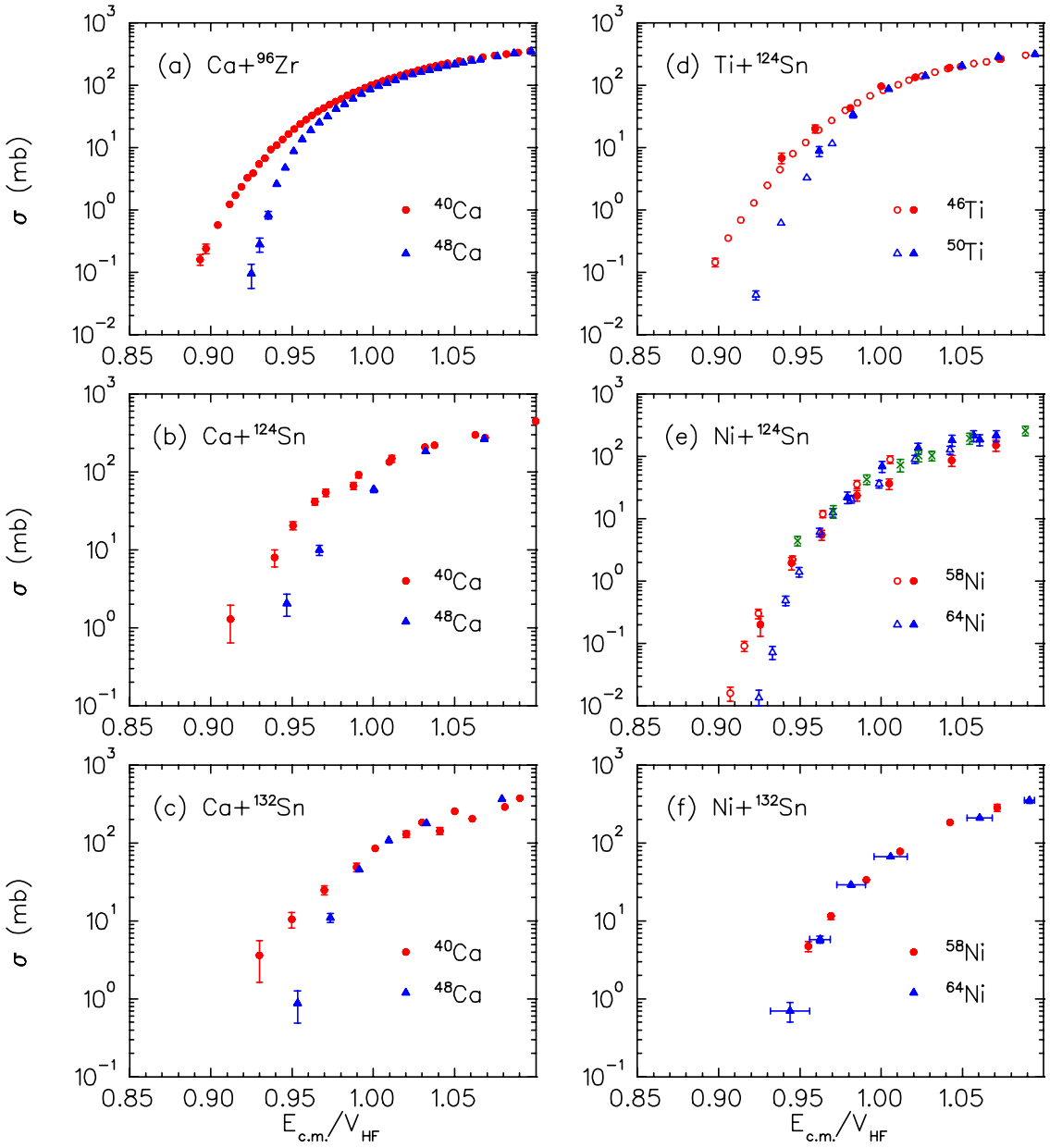

FIG. 5: (Color online) Comparisons of reduced fusion excitation functions for (a) ^{40,48}Ca+^{96}Zr, (b) ^{40,48}Ca+^{124}Sn, (c) ^{40,48}Ca+^{132}Sn, (d) ^{46,50}Ti+^{124}Sn, (e) ^{58,64}Ni+^{124}Sn, and (f) ^{58,64}Ni+^{132}Sn. The data points shown by the crosses in (e) are for ^{64}Ni+^{118}Sn. The reduced energy is obtained by dividing the center-of-mass energy by the barrier height predicted by the frozen Hartree-Fock method.

The excitation functions for ^{50}Ti+^{124}Sn and ^{48}Ca+^{124}Sn overlap with each other. As mentioned above, the Q-values for neutron transfer are negative for both reactions. The sub-barrier fusion enhancement for ^{46}Ti+^{124}Sn is larger than ^{50}Ti+^{124}Sn which correlates with the presence of positive Q-values for neutron transfer. On the other hand, the enhancement for ^{46}Ti+^{124}Sn is smaller than ^{40}Ca+^{124}Sn until $E_{c.m.}/V_{HF}$=0.92 and the cross section for ^{46}Ti+^{124}Sn decreases with energy more slowly than for ^{40}Ca+^{124}Sn.

In order to better understand the reaction mechanisms, the barrier distributions for

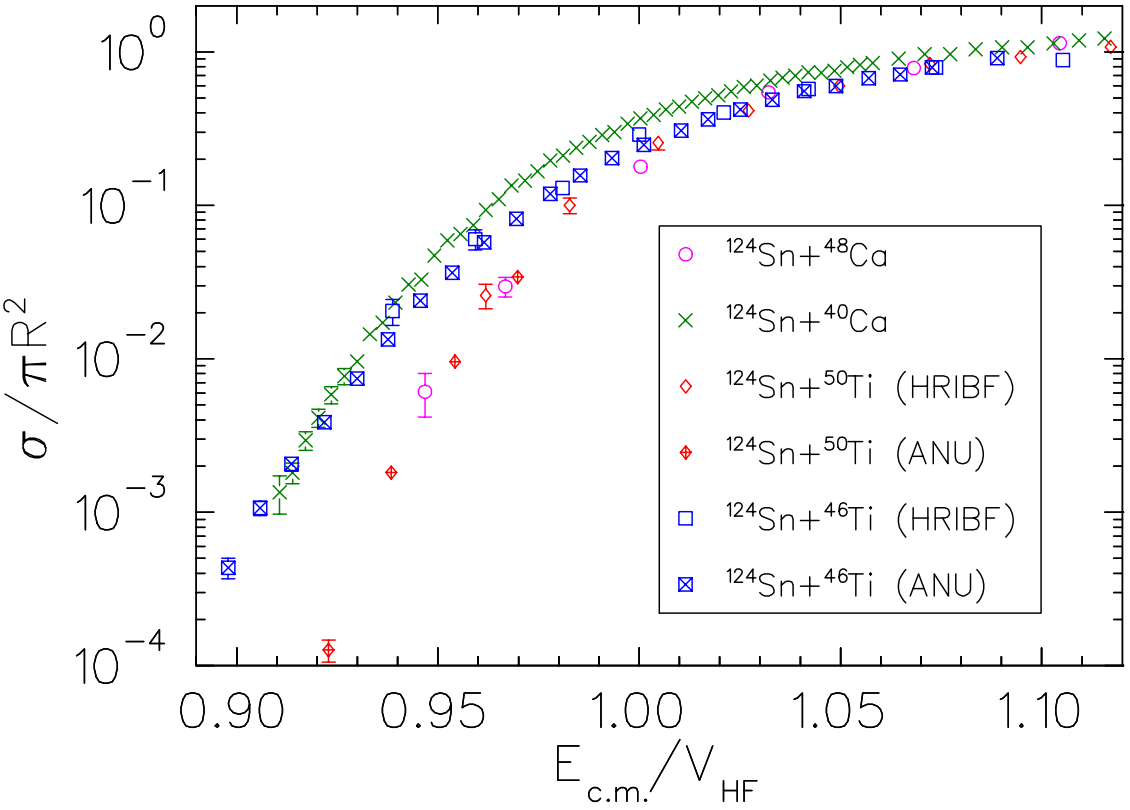

FIG. 6: (Color online) Comparison of the reduced fusion excitation functions for ^{40}Ca+^{124}Sn [7] (crosses), ^{48}Ca+^{124}Sn [5] (circles), ^{50}Ti+^{124}Sn (triangles), and ^{46}Ti+^{124}Sn (squares and diamonds).

^{40}Ca+^{124}Sn [7] and ^{46}Ti+^{124}Sn were obtained by taking the second derivative of the product of the cross section and energy using the point difference formula [29]. The barrier distributions are compared in Fig. 7. For both systems, the barrier strength is generally below the calculated frozen HF barrier, $E_{c.m.}/V_{HF} = 1$, as would be expected since the frozen HF predictions are for "bare" barriers that do not include any coupling effects. This barrier strength at low energies in the experimental barrier distribution is responsible for fusion enhancement at sub-barrier energies. The low-energy tail of the barrier distributions for ^{46}Ti+^{124}Sn and ^{40}Ca+^{124}Sn has shallower slopes. This is associated with coupling to transfer channels with positive Q-values. Nevertheless, for ^{40}Ca+^{124}Sn, the centroid of the barrier distribution at the lowest energies lies 5% below the uncoupled barrier which is lower than that for ^{46}Ti+^{124}Sn, 3% below the uncoupled barrier. As a result, the sub-barrier fusion enhancement for ^{40}Ca+^{124}Sn is larger.

The extent of the sub-barrier fusion enhancement is different for ^{40}Ca+^{124}Sn, ^{46}Ti+^{124}Sn, and ^{58}Ni+^{124}Sn although the Q-values for transferring two to five neutrons are similar, as shown in Fig. 1. It is instructive to compare the barrier distributions deduced from the CCFULL calculations for these reactions to investigate whether there are differences in the contributions from coupling to inelastic excitations. Since all three reactions involve a common nucleus, ^{124}Sn, the couplings to the collective excitations in ^{40}Ca, ^{46}Ti, and ^{58}Ni are examined first. For the reaction involving ^{40}Ca, the result of the weak coupling to the lowest 2^+ state leads to the main barrier strength being just below the uncoupled barrier, as shown by the dotted curve in Fig. 8(a). The stronger coupling to the 3^- state in ^{40}Ca

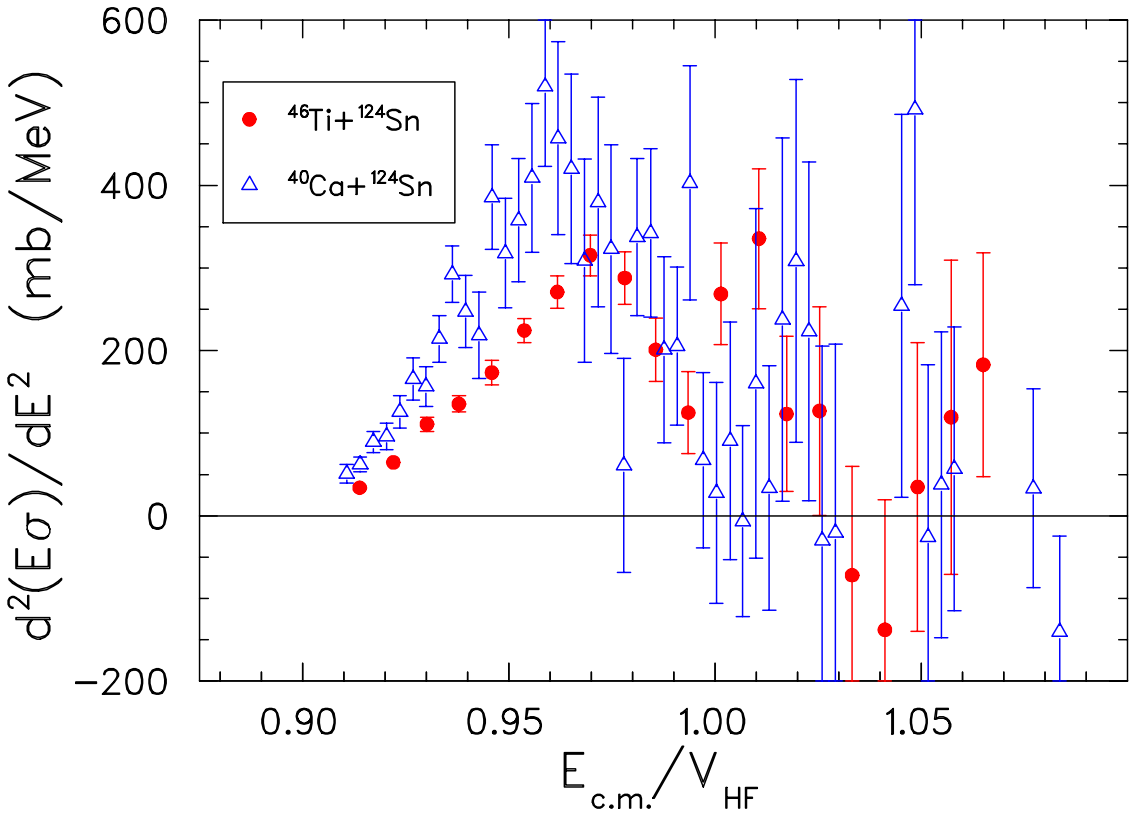

FIG. 7: (Color online) Comparison of barrier distributions for ^{40}Ca+^{124}Sn [7] (triangles) and ^{46}Ti+^{124}Sn (circles) obtained from the measured fusion excitation functions.

produces a much larger change, with the centroid of the resulting low-energy peak in the barrier distribution being 3.5% below the uncoupled barrier. The barrier distribution at energies below the uncoupled barrier is very similar for couplings to both 2^+ and 3^- and 3^- alone, showing that the coupling to the 3^- state is dominant, as shown in Fig. 8(a). It is worth noting that the coupling to the octupole state in ^{40}Ca also results in a barrier well below the uncoupled barrier for other reactions [31–33].

For the ^{46}Ti induced reaction, the weak coupling to the 3^- state leads to a peak in the barrier distribution with its centroid slightly lower than the uncoupled barrier. The strong coupling to the 2^+ state results in a peak in the barrier distribution 2.5% below the uncoupled barrier. By including both the 2^+ and 3^- states in the coupled-channels calculation, the barrier distribution at low energies is shifted slightly lower.

For the reaction involving ^{58}Ni, the coupling to the 2^+ and 3^- states each leads to a peak in the barrier distribution at the same location below the uncoupled barrier but with different probabilities. Including both states in the calculation results in shifting the lowest peak further to 3% below the uncoupled barrier.

Next, couplings to the states in the target, in addition to the couplings to states in the projectile discussed above, are included. Couplings to the 2^+ and 3^- states in ^{124}Sn shifts the low-energy peaks in the barrier distributions to slightly lower energies, as can be seen in Fig. 8. Comparing the calculated barrier distributions for the three systems, it is clear that ^{40}Ca+^{124}Sn system has a large strength at low energies, followed by ^{58}Ni+^{124}Sn and finally ^{46}Ti+^{124}Sn. Thus, if transfer couplings were not playing a significant role, then

the sub-barrier fusion enhancement for ^{40}Ca+^{124}Sn would be expected to be the largest followed by ^{58}Ni+^{124}Sn and ^{46}Ti+^{124}Sn. Experimentally, whilst ^{40}Ca+^{124}Sn has the largest enhancement, the enhancement for ^{46}Ti+^{124}Sn is larger than that for ^{58}Ni+^{124}Sn. For both ^{40}Ca+^{124}Sn and ^{46}Ti+^{124}Sn, the experimental barrier distributions extend well below the calculated ones and the strength at lowest energies falls off very slowly. This would be expected if many positive Q-value transfer channels were playing a role. Barrier distributions are not available for ^{58}Ni+^{124}Sn, which makes it difficult to make further statements about the reduced enhancement compared to ^{40}Ca+^{124}Sn and ^{46}Ti+^{124}Sn.

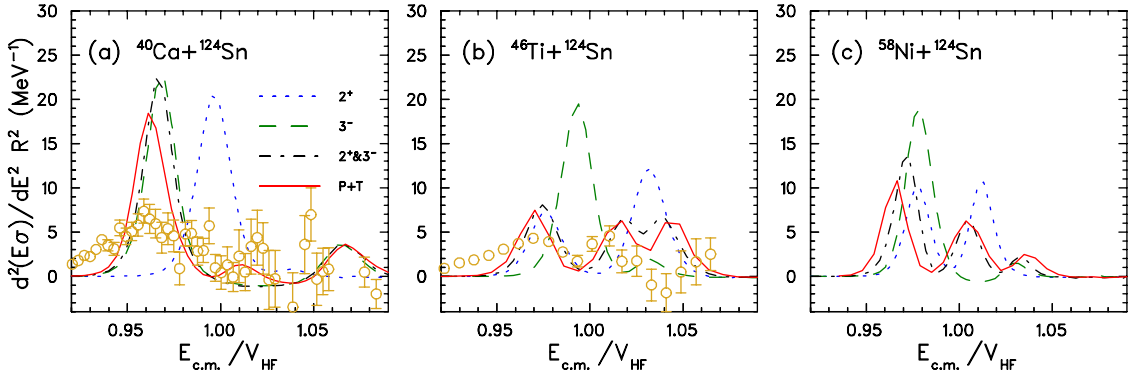

FIG. 8: (Color online) (a) Reduced barrier distributions for ^{40}Ca+^{124}Sn calculated by the coupled-channels code CCFULL. The dotted curve is for coupling to the 2^+ state, the dashed curve is for coupling to the 3^- state, the dash-dotted curve is for coupling to the 2^+ and 3^- states in ^{40}Ca, and the solid curve is for coupling to the 2^+ and 3^- in ^{40}Ca and ^{124}Sn. The experimental data are shown by the open circles. (b) ^{46}Ti+^{124}Sn. (c) ^{58}Ni+^{124}Sn.

Implementing realistic coupling for neutron transfer in coupled-channels calculations is a very challenging theoretical problem. In the cases that involve transferring multiple nucleons and populating many states, the task is even more difficult. By comparing the coupling to inelastic excitations of the projectile and target among the three reactions, this analysis suggests that the large sub-barrier fusion enhancement in ^{40}Ca+^{124}Sn is the result of coupling to both transfer and inelastic excitation, with coupling to the 3^- state in ^{40}Ca playing the major role.

Besides ^{40}Ca induced reactions, a very large sub-barrier fusion enhancement has been reported for ^{32}S induced reactions [35, 36]. As an example, the sub-barrier fusion enhancement in ^{32}S+^{110}Pd is much larger than that in ^{36}S+^{110}Pd. Similar to the comparison between ^{40}Ca+^{124}Sn and ^{48}Ca+^{124}Sn, the large sub-barrier fusion enhancement in ^{32}S+^{110}Pd is attributed to the coupling to transfer because there are neutron transfer channels with positive Q-values in ^{32}S+^{110}Pd [35]. However, in the slightly heavier ^{40}Ar induced fusion, there is no difference in the shape of the excitation functions between ^{40}Ar+^{112}Sn and ^{40}Ar+^{122}Sn even though the Q-value for two-neutron transfer is positive in ^{40}Ar+^{122}Sn [37, 38]. It is worth noting that ^{32}S has a very collective high-lying octupole state, like ^{40}Ca. It is likely that the coupling to the octupole state in ^{32}S substantially enhance fusion induced by ^{32}S at sub-barrier energies.

For reactions with a large $Z_P Z_T$, the coupling to inelastic excitations contributes significantly to sub-barrier fusion enhancement. This may make the contributions from coupling to transfer seem less important. As seen in the comparison for ^{58,64}Ni+^{124}Sn, the excitation functions do not differ until the cross section is less than 1 mb. In contrast, the influence

of neutron transfer seems to be more significant for lighter systems. Whether the fusion of lighter nuclei occurring in the crust of neutron stars would be enhanced by transfer, as predicted by TDHF [3], would be interesting for further research. Moreover, it is not known if the large collectivity in one of the participating nuclei would make the effect of coupling to transfer more pronounced, as seen in ^{40}Ca induced fusion. This observation could be important for using neutron-rich radioactive beams for superheavy element synthesis. Perhaps, the production rate would be higher when one or both of the nuclei in the reaction have a large inelastic excitation probability.

V. CONCLUSIONS

Fusion excitation functions for ^{46,50}Ti+^{124}Sn have been measured in an attempt to resolve the differences in sub-barrier fusion enhancement observed in ^{40,48}Ca+^{124,132}Sn and ^{58,64}Ni+^{124,132}Sn. In particular, the fusion cross sections for ^{46}Ti+^{124}Sn were measured to high precision and in fine steps to allow determination of the barrier distribution for comparison with the previously published ^{40}Ca+^{124}Sn data. It is found that there is a peak in the barrier distribution below the uncoupled barrier. For ^{40}Ca+^{124}Sn, the peak is further below the uncoupled barrier than that for ^{46}Ti+^{124}Sn. Coupled-channels calculations including the inelastic excitation of the projectile and target show similar behaviors. The coupling to inelastic excitations and neutron transfer is likely to be the reason for the very large sub-barrier fusion enhancement in ^{40}Ca+^{124}Sn with the coupling to the octuple state in ^{40}Ca playing a major role. To further probe the effects of transfer couplings on sub-barrier fusion in ^{46}Ti+^{124}Sn, it would be necessary to measure multineutron transfer cross sections to deduce the transfer form factors and compare with the results for ^{40}Ca+^{124}Sn [39]. Further work is also needed to clarify the effect of charged particle transfer, as well as neutron transfer, in fusion of heavy systems such as Ni+Sn.

VI. ACKNOWLEDGMENTS

This material is based upon work supported by the U.S. Department of Energy, Office of Science, Office of Nuclear Physics and this research used resources of the Holifield Radioactive Ion Beam Facility of Oak Ridge National Laboratory, which was a DOE Office of Science User Facility. Research at ANU was supported by the Australian Research Council Grants DP130101569, FT120100760, DP140101337, FL110100098, DE140100784 and by NCRIS for the operation of the Heavy Ion Accelerator Facility.

[1] L.F. Canto, P.R.S. Gomes, J. Lubian and M.S. Hussein, EPJ Web of Conferences **17**, 01001 (2011).
[2] W. Loveland, Phys. Rev. C. **76**, 014612 (2007).
[3] A.S. Umar, V.E. Oberacker, and C.J. Horowitz, Phys. Rev. C **85**, 055801 (2012).
[4] C.J. Horowitz, H. Dussan, and D.K. Berry, Phys. Rev. **77**, 045807 (2008).
[5] J.J. Kolata, A. Roberts, A.M. Howard, D. Shapira, J.F. Liang, C.J. Gross, R.L. Varner, Z. Kohley, A.N. Villano, H. Amro, W. Loveland, and E. Chavez, Phys. Rev. C **85**, 054603 (2012).

[6] Z. Kohley, J.F. Liang, D. Shapira, C.J. Gross, R.L. Varner, J.M. Allmond, J.J. Kolata, P.E. Mueller, and A. Roberts, Phys. Rev. C **87**, 064612 (2013).
[7] F. Scarlassara, S. Beghini, G. Montagnoli, G.F. Segato, D. Ackermann, L. Corradi, C.J. Lin, A.M. Stefanini, L.F. Zheng, Nucl. Phys. **A672**, 99 (2000).
[8] H. Timmers, D. Ackermann, S. Beghini, L. Corradi, J.H. He, G. Montagnoli, F. Scarlassara, A.M. Stefanini, N. Rowley, Nucl. Phys. **A633**, 421 (1998).
[9] A.M. Stefanini, B.R. Behera, S. Beghini, L. Corradi, E. Fioretto, A. Gadea, G. Montagnoli, N. Rowley, F. Scarlassara, S. Szilner, and M. Trotta, Phys. Rev. C **76**, 014610 (2007).
[10] Z. Kohley, J.F. Liang, D. Shapira, R.L. Varner, C.J. Gross, J.M. Allmond, A.L. Caraley, E.A. Coello, F. Favela, K. Lagergren, and P.E. Mueller, Phys. Rev. Lett. **107**, 202701 (2011).
[11] J.F. Liang, D. Shapira, J.R.Beene, C.J. Gross, R.L. Varner, A. Galindo-Uribarri, J. Gomez del Campo, P.A. Hausladen, P.E. Mueller, D.W. Stracener, H. Amro, J.J. Kolata, J.D. Bierman, A.L. Caraley,K.L. Jones, Y. Larochelle, W. Loveland, and D. Peterson, Phys. Rev. C **75**, 054607 (2007).
[12] K.T. Lesko, W. Henning, K.E. Rehm, G. Rosner, J.P. Schiffer, G.S.F. Stephans, B. Zeidman, and W.S. Freeman, Phys. Rev. C **34**, 2155 (1986).
[13] C.L. Jiang, A.M. Stefanini, H. Esbensen, K.E. Rehm, S. Almaraz-Calderon, M.L. Avila, B.B. Back, D. Bourgin, L. Corradi, S. Courtin, E. Fioretto, F. Galtarossa, A. Goasduff, F. Haas, M.M. Mazzocco, D. Montanari, G. Montagnoli, T. Mijatovic, R. Sagaidak, D. Santiago-Gonzalez, F. Scarlassara, E.E. Strano, and S. Szilner, Phys. Rev. C **91**, 044602 (2015).
[14] F.L.H. Wolfs, Phys. Rev. C **36**, 1379 (1987).
[15] J.D. Bierman, P. Chan, J.F. Liang, M.P. Kelly, A.A. Sonzogni, R. Vandenbosch, Phys. Rev. Lett. **76**, 1587 (1996).
[16] N.G. Nicolis and J.R. Beene, a multi-particle Monte Carlo evaporation code (1993), unpublished.
[17] D. Shapira, J.F. Liang, C.J. Gross, R.L. Varner, H. Amro, C. Harlin, J.J. Kolata, and S. Novotny, Nucl. Instrum. Methods Phys. Res., Sect. A **551**, 330 (2005).
[18] M.D. Rodrígues, M.L. Brown, M. Dasgupta, D.J. Hinde, D.C. Weisser, T. Kibèdi, M.A. Lane, P.J. Cherry, A.G. Muirhead, R.B. Turkentine, N. Lobanov, A.K. Cooper, A.B. Harding, M. Blacksell, P.M. Davidson, Nucl. Instrum. Methods Phys. Res., Sect. A **614**, 119 (2010).
[19] SOLIX, unpublished.
[20] A. Mukherjee, M. Dasgupta, D.J. Hinde, K. Hagino, J.R. Leigh, J.C. Mein, C.R. Morton, J.O. Newton, and H. Timmers, Phys. Rev. C **66**, 034607 (2002).
[21] K. Hagino, N. Rowley, and A.T. Kruppa, Comput. Phys. Commun. **123**, 143 (1999).
[22] R.A. Broglia and A. Winther, *Heavy Ion Reactions*, Frontiers in Physics Lecture Series, Vol. 84 (Addison-Wesley, Redwood, CA, 1991).
[23] R. Bass, Nucl. Phys. A **231**, 45 (1974).
[24] L.C. Chamon, Nucl. Phys. A **787**, 198 (2007).
[25] S.-K. Ma and K.A. Brueckner, Phys. Rev. **165**, 18 (1968).
[26] A.M. Stefanini, F. Scarlassara, S. Beghini, G. Montagnoli, R. Silvestri, M. Trotta, B.R. Behera, L. Corradi, E. Fioretto, A. Gadea, Y.W. Wu, S. Szilner, H.Q. Zhang, Z. H. Liu, M. Ruan, F. Yang, and N. Rowley, Phys. Rev. C 73, 034606 (2006).
[27] S. Raman, C.W. Nestor, and P. Tikkanen, At. Data Nucl. Data Tables **36**, 1 (1987).
[28] T. Tibédi and R.H. Spear, At. Data Nucl. Data Tables **80**, 35 (2002).
[29] M. Dasgupta, D. Hinde, N. Rowley, A. Stefanini, Annu. Rev. Nucl. Part. Sci. **48**, 401 (1998).
[30] H.K. Kim, T. Otsuka, and P. Bonche, J. Phys. G: Nucl. Part. Phys. **23**, 1267 (1997).

[31] K. Hagino, N. Takigawa, M. Dasgupta, D.J. Hinde, and J.R. Leigh, Phys. Rev. Lett. **79**, 2014 (1997).
[32] M. Trotta, A.M. Stefanini, L. Corradi, A. Gadea, F. Scarlassara, S. Beghini, and G. Montagnoli, Phys. Rev. C **65**, 011601(R), (2001).
[33] C. Simenel, M. Dasgupta, D.J. Hinde, and E. Williams, Phys. Rev. C **88**, 064604 (2013).
[34] A.M. Stefanini, G. Fortuna, R. Pengo, W. Meczynski, G. Montagnoli, L. Corradi, A. Tivelli, S. Beghini, C. Signorini, S. Lunardi, M. Morando, and F. Soramel, Nucl. Phys. **A456**, 509 (1986).
[35] A.M. Stefanini, D. Ackermann, L. Corradi, J.H. He, G. Montagnoli, S. Beghini, F. Scarlassara, and G.F. Segato, Phys. Rev. C **52**, R1727 (1995).
[36] H.Q. Zhang, C.J. Lin, F. Yang, H.M. Jia, X.X. Xu, Z.D. Wu, F. Jia, S.T. Zhang, Z.H. Liu, A. Richard, and C. Beck, Phys. Rev. C **82**, 054609 (2010).
[37] A.M. Stefanini, J. Phys. G **23**, 1401 (1997).
[38] W. Reisdorf, F.P. Hessberger, K.D. Hildenbrand, S. Hofmann, G. Münzenberg, K.-H. Schmidt, J.H.R. Schneider, W.F.W. Schneider, K. Sümmerer, G. Wirth, J.V. Kratz, K. Schlitt, Nucl. Phys. **A438**, 212 (1985).
[39] L. Corradi, J.H. He, D. Ackermann, A.M. Stefanini, A. Pisent, S. Beghini, G. Montagnoli, F. Scarlassara, G.F. Segato, G. Pollarolo, C.H. Dasso, and A. Winther, Phys. Rev. C **54**, 201 (1996).